

# Impact of multiple launches on initial disturbances of unguided rockets

Hossam Eisa<sup>1</sup>, Mahmoud Y M mohamed<sup>2</sup>, Sherief Saleh<sup>3</sup> and Mostafa Khalil<sup>4</sup>

<sup>1</sup> M.Sc., Aerospace Engineering Department, Military Technical College, Egypt

<sup>2</sup> Professor, Aerospace Engineering Department, Military Technical College, Egypt

<sup>3</sup> Assistant Professor, Aerospace Engineering Department, Military Technical College, Egypt

<sup>4</sup> Associate Professor, Aerospace Engineering Department, Military Technical College, Egypt  
hossameisa@mtc.edu.eg

**Abstract.** Dispersion is a key aspect as for as unguided rockets are concerned. Whether it is desired (for large area coverage) or not (for higher localized impact), dispersion should however, initial (launch) dispersion are a major factor. These disturbances become more pronounced, more sophisticated, and harder to investigate in case of multiple launches. This study investigates the dynamic behavior of a wheeled rocket launcher equipped with vertically aligned launch tubes, analyzing the impact of successive rocket firings on the rockets' initial disturbances influencing their dispersion. The launcher system is modeled as a multibody system using the transfer matrix method (TMM), allowing for a simple approach by bypassing the typical manipulation of sophisticated dynamic equations. This approach is validated by comparison with results obtained using Lagrange's equations proposed in the literature, ensuring model reliability and accuracy. The analysis includes a comprehensive examination of the dynamic interactions between the launcher canister and the vehicle chassis, providing insight into how different components of the system respond to the action of sequential firings. Findings underscore the importance of optimal selection and configuration of launcher components to mitigate negative impacts on vehicle stability and rocket dispersion.

## 1. Introduction

The Multiple Launch Rocket System (MLRS) is extensively utilized globally due to its numerous advantages and benefits [1]. An advantage of MLRS is its high firing rate, by sequentially launching a massive number of rockets in a short period. Rocket launchers including MLRS consist of various components as depicted in Figure 1, to be considered as multibody systems [2]. The dynamics of these launch systems have a significant impact on the rocket initial disturbance and hence its trajectory thus having a significant impact on the unguided rocket dispersion[3]. The launcher dynamics are greatly influenced by the time intervals between successive shots and the firing sequence in MLRS, which have a great effect on the initial disturbance of the rocket at the muzzle. It is important to understand the dynamic behavior of these launchers and determine the time interval between shots to maximize effectiveness and passively control the resulting disturbances generated during rocket launches.

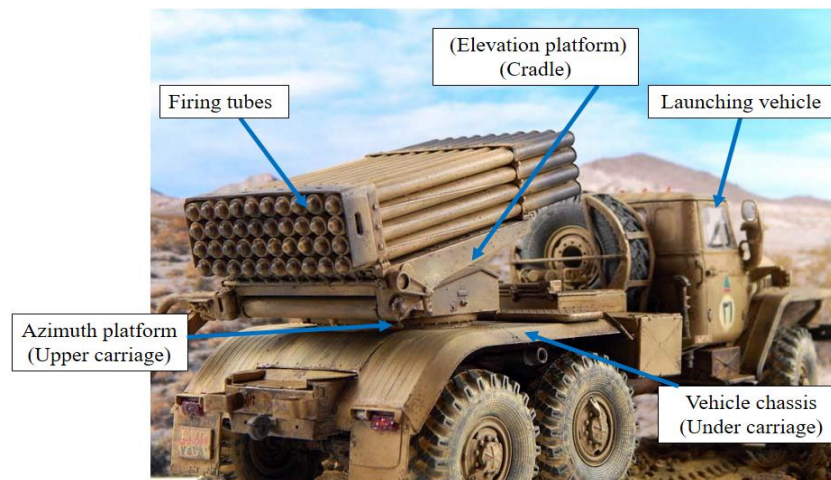


**Figure 1.** MLRS components.

Several methods have been proposed for modeling rocket launch systems, particularly MLRS to understand its complex behavior. Newton-Euler method is a widely used technique in this field. The equations of motion for MLRS were derived by Cochran [4, 5] using the Newton-Euler method. A dynamic model was developed including two rigid bodies, namely the launcher and the rocket. Another study [6] was developed to simulate the dynamics of MLRS during successive launching of rockets. In other studies [7, 8], the authors employed the Newton-Euler method to simulate the dynamic behavior of MLRS, specifically aimed at designing a controller for the azimuth and elevation mechanisms. Another notable approach employed in the dynamic modeling of rocket launch systems is the Lagrange method [9-11].

Rui et al [10, 11], established a mathematical model of MLRS based on the Lagrange equation of motion in. The main objective for developing this model was to design a PID controller to control the orientation of the system components and maintain the launcher parts on target using the concept of torque control. Another study [12] employed the Lagrange method in modeling a wheeled rocket launcher, applying five generalized coordinates and five inertia components to study the dynamic behavior of the launcher and its components. The vehicle was modelled as half car model to simplify the model.

Recently, Rui and his group developed TMM [13] and its modified version [14], which simplifies intricate computations and lowers computational costs, offer considerable benefits for the dynamic modeling of rocket launchers and MLRS. In [15] a dynamic model of MLRS was developed to design an active controller to regulate the launcher motion, and decrease the vibration of the launcher during firing. The model is composed of twenty four elements divided into rigid bodies, lumped masses, and elastic elements. A dynamical mathematical model of MLRS was developed in [16] to solve the problem of dynamic design of MLRS. The launcher included eighteen firing tubes mounted on the vehicle. The dynamic model of the launcher with the vehicle is composed of twenty-eight elements including rigid bodies and elastic elements. In [17] and [18] a dynamical mathematical model of MLRS was developed based on the new version of TMM for the same case study in [16]. The main purpose of this study was to investigate the dynamic behavior of MLRS as a multibody system and study the effect of launcher dynamics on rocket dispersion. The updated version of TMM was utilized in [19] to create a dynamic of the same launcher in [12]. A parametric research was performed to comprehend the dynamic characteristics of the launcher under operating conditions.

In this study, a dynamic model of a simplified rocket launch system composed of five vertically arranged tubes mounted on a wheeled vehicle [12] is developed using TMM [14]. The overall transfer matrix is derived using the automatic deduction theorem [20]. To confirm the validity of the model, comparisons are made with results from the literature [12] that utilized the Lagrange method. Multiple rocket launches with varying time intervals between successive shots are examined to study the effects

of the repeated launches on the linear and angular motion of the system components as well as the initial disturbances of the unguided rockets.

## 2. Case study

The single tube launcher mounted on a vehicle proposed in [12] serves as a case study for validation purposes. The half-car model [21] was employed to represent the vehicle, facilitating the analysis and understanding of the suspension system characteristics, as illustrated in Figure 2. Subsequently, the single tube launcher is replaced with a canister of five tubes as shown in Figure 3.

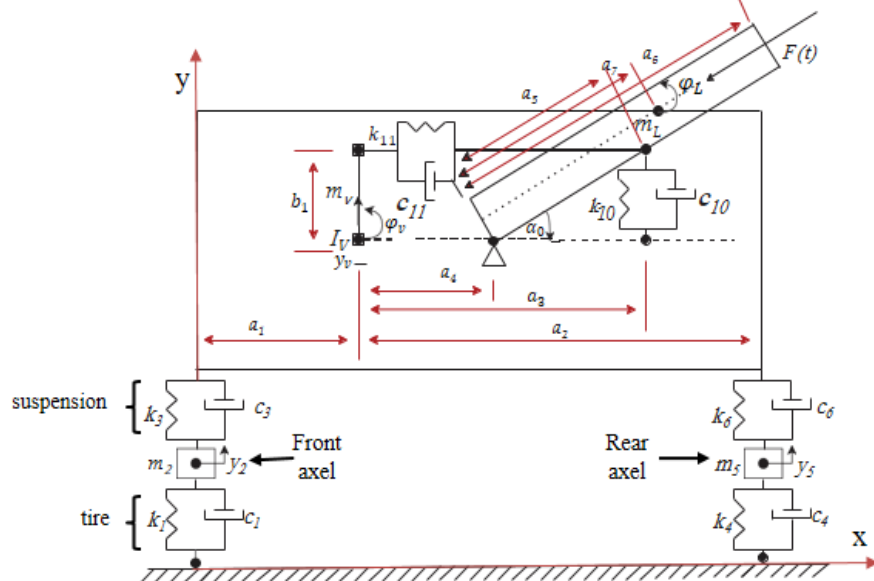


Figure 2. Dynamic model of single tube launcher [12].

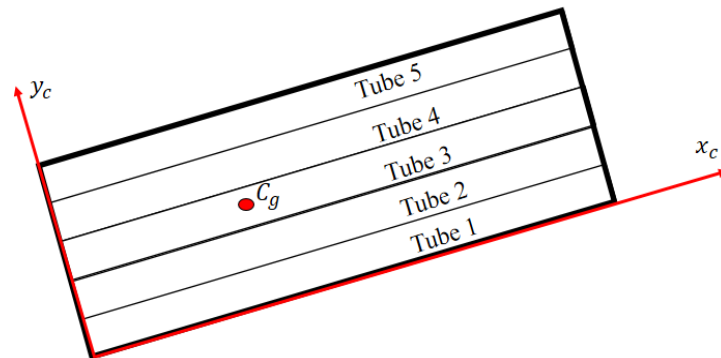


Figure 3. Canister of five tubes.

Lagrange differential equation is employed in the proposed model [12] to develop the dynamical mathematical model of five generalized coordinates ( $y_2, y_5, y_v, \varphi_v, \varphi_L$ ) and five inertia components ( $m_2, m_5, m_v, m_L, I_v$ ).  $F(t)$  is the generalized force describing the rocket excitation force on the launcher. For additional information regarding the parameters in Figure 2, please refer to [12]. The launcher is mounted on the vehicle by two elastic elements each one characterized by a damping and stiffness coefficient ( $k_{10}, k_{11}, c_{10}, c_{11}$ ) with the values of  $k_{10} = k_{11} = 22 \text{ KN/m}$  and  $c_{10} = c_{11} = 20 \text{ KN.s/m}$ . The angle  $\alpha_0$  represents the angle between the horizontal and the launcher. Some physical parameters of the vehicle and the launcher tubes with the rockets are presented in Table 1. The mass centers of the vehicle and the launcher are measured from the input point of each part. The

parameters of each body are displayed in the respective body-fixed frame. The mass of the rocket  $m_R$  in the analysis is 66 kg and the thrust  $F_R$  is 23600 N [22].

**Table 1.** Some physical parameters of the system

	Front-wheel	Rear-wheel	Vehicle chassis	launcher	
				One tube	Five tubes
Mass, [kg]	755	1550	3600	80	426.1
Mass center [m]	(0,0)	(0,0)	(2.94,0)	(0.82,0)	(1.34,0.31)
Moment of inertia, $I_{zz}$ , [kg.m <sup>2</sup> ]	0	0	60000	128	865

### 3. Mathematical model

The modified version of TMM proposed in [14] is employed to establish the dynamic model of the vehicle launcher system. Figure 4 illustrates the topology diagram of the dynamic model. The system is classified into hinge elements and body elements. According to the topology diagram, the boxes refer to the body elements and the arrows refer to the hinge elements. The arrow direction indicates the transfer direction. The hinge element mass is negligible [17]. Every element of the system is designated a number from one to eleven. The whole front and rear axles are considered as lumped masses, assigned to numbers 2 and 5, respectively. The launcher and the vehicle chassis are considered rigid bodies, designated the numbers 9 and 7, respectively. The hinge elements have the numbers 1, 3, 4, 6, 8, 10, 11. The number 0 represents the system boundaries.

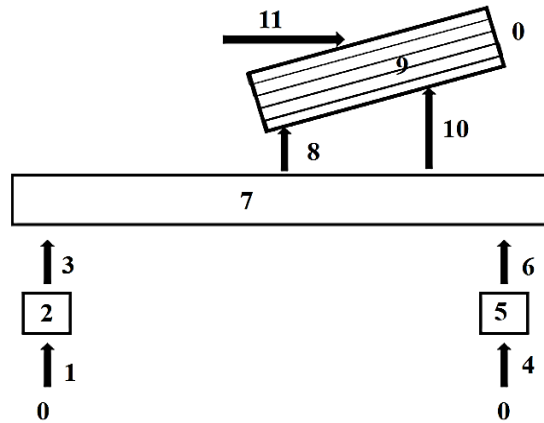


**Figure 4.** Model topology of the launcher vehicle system.

#### 3.1. State vector and transfer equation

As the system moves in the plane, the state vector "Z" comprises seven elements as represented in equation (1).

$$Z = [\ddot{x} \quad \ddot{y} \quad \dot{\Omega}_z \quad m_z \quad q_x \quad q_y \quad 1]^T \quad (1)$$

where  $\ddot{x}$  and  $\ddot{y}$ , are the linear accelerations related to  $q_x$  and  $q_y$ , respectively.  $\dot{\Omega}_z$  represents the angular acceleration corresponding to the torque  $m_z$ . Equation (2) represents the relation between the output and the input state vector and is denoted by the transfer equation of the entire element.

$$Z_{k,O} = M_K Z_{k,I} \quad (2)$$

where  $M_K$  is the element k transfer matrix and it is a 7x7 square matrix. The element k input and output state vectors are represented by  $Z_{k,I}$  and  $Z_{k,O}$ , respectively.

#### 3.2. Transfer matrices

Elements 2 and 5 are treated as lumped masses with a single input and a single output. Element 9 is defined as a rigid body with a single input and a single output. The elements 2, 5, and 9 transfer

equations are the same as equation (2). Element 7 has two inputs and one output and its transfer equation is represented in equation (3).

$$Z_{7,0} = M_{7,I_1}Z_{I_1} + M_{7,I_2}Z_{I_2} \quad (3)$$

where,  $Z_{I_1}$  and  $Z_{I_2}$  are the two input state vectors of vehicle 7.  $M_{7,I_1}$  is the rigid body transfer matrix and can be found in [14] and represented as,

$$M_{7,I_1} = \begin{bmatrix} I_2 & C_1 & 0_{2 \times 1} & 0_{2 \times 2} & C_2 \\ 0_{1 \times 2} & 1 & 0 & 0_{1 \times 2} & 0 \\ C_6C_3 + C_7 & C_6C_4 + C_8 & 1 & C_6 & C_6C_5 + C_9 \\ C_3 & C_4 & 0_{2 \times 1} & I_2 & C_5 \\ 0_{1 \times 2} & 0 & 0 & 0_{1 \times 2} & 1 \end{bmatrix} \quad (4)$$

The moments and forces from the second input state vector  $Z_{I_2}$  are obtained by the extraction matrix [20]  $M_{7,I_2}$  and represented as,

$$M_{7,I_2} = \begin{bmatrix} 0_{2 \times 2} & 0_{2 \times 1} & 0_{2 \times 1} & 0_{2 \times 2} & 0_{2 \times 1} \\ 0_{1 \times 2} & 0 & 0 & 0_{1 \times 2} & 0 \\ 0_{1 \times 2} & 0 & 1 & r_{I_2,0} & 0 \\ 0_{2 \times 2} & 0_{2 \times 1} & 0_{2 \times 1} & I_2 & 0 \\ 0_{1 \times 2} & 0 & 0 & 0_{1 \times 2} & 1 \end{bmatrix} \quad (5)$$

In comparison to algebraic equations, equation (3) has more unknowns. Therefore the geometric equation (6) is employed.

$$H_{7,I_1}Z_{I_1} = H_{7,I_2}Z_{I_2} \quad (6)$$

where  $H_{7,I_1}$  and  $H_{7,I_2}$  are depicted in references [17] and [20].

Simultaneously, elements 1, 3, 4, 6, and 8 are considered to be elastic and acceleration hinges in parallel [17]. Utilizing the elastic hinge allows for the modeling of the damping and elastic forces that exist between two bodies [14]. The acceleration hinge does not link the two bodies; rather, it serves to facilitate the transfer equation and is illustrated in equation (7).

$$M_{\text{acceleration hinge}} = \begin{bmatrix} 0_{3 \times 3} & -\hat{s}_1^{-1}\hat{s}_2 & -\hat{s}_1^{-1}\hat{s}_3 \\ 0_{3 \times 3} & I_3 & 0_{3 \times 1} \\ 0_{1 \times 3} & 0_{1 \times 3} & 1 \end{bmatrix} \quad (7)$$

### 3.3. The system overall transfer matrix equation

Given the system topology and the automatic deduction theory [20], the system transfer equation is as follows

$$M_{\text{all}}Z_{\text{all}} = 0 \quad (8)$$

where,

$$M_{\text{all}} = \begin{bmatrix} -I_7 & R_{1-9} & R_{4-9} \\ 0_{4 \times 7} & Q_{1-7} & Q_{4-7} \end{bmatrix} \quad (9)$$

where,

$$\begin{aligned} R_{1-9} &= M_9M_8M_{7,I_1}M_3M_2M_1 \\ R_{4-9} &= M_9M_8M_{7,I_2}M_6M_5M_4 \\ Q_{1-7} &= -H_{7,I_1}M_3M_2M_1 \\ Q_{4-7} &= H_{7,I_2}M_6M_5M_4 \end{aligned} \quad (10)$$

$Z_{\text{all}}$  is the vector comprised of the boundary state vectors and shown in equation (11).

$$Z_{\text{all}} = [Z_{9,0}^T \quad Z_{1,0}^T \quad Z_{4,0}^T] \quad (11)$$

The boundary condition of the vehicle launcher system is illustrated as,

$$\begin{aligned} Z_{9,0} &= [\ddot{x} \quad \ddot{y} \quad \dot{\Omega}_z \quad 0 \quad 0 \quad 0 \quad 1]^T_9 \\ Z_{1,0} &= [0 \quad 0 \quad 0 \quad m_z \quad q_x \quad q_y \quad 1]^T_1 \end{aligned} \quad (12)$$

$$Z_{4,0} = [0 \ 0 \ 0 \ m_z \ q_x \ q_y \ 1]^T_4$$

The boundary state vector unknown variables can be determined by inserting the specified boundary condition into equations (11) and (8), subsequently eliminating the identified boundary variables.yields:

$$\bar{M}_{all}\bar{Z}_{all} = 0 \quad (13)$$

$\bar{Z}_{all}$  denotes the reduced overall state vector after the exclusion of identified boundary variables, whereas  $\bar{M}_{all}$  signifies the reduced overall matrix. Equation (2) can be used to obtain the entire state vectors of the system.

### 3.4. Rocket acceleration and loads

During the launch process, the acceleration of the rocket and the normal reaction that the rocket exerts on the tube are both defined by equations (14) and (15), respectively.

$$m_R \ddot{x}_R = F_R - N(\sin \alpha + f \cos \alpha) \quad (14)$$

$$N = \frac{I_R F_R \tan \alpha}{m_R r^2} \quad (15)$$

where,  $N$  is the reaction normal to the tube,  $\alpha$  is the helix angle of the tube,  $\ddot{x}_R$  is the acceleration of the rocket during its motion in the tube,  $I_R$  is the mass moment of inertia of the rocket,  $r$  is the radius of the rocket, and  $f$  is the coefficient of friction between the rocket and tube. The following equation can be used to determine the influence of rocket dynamics on the launching tubes.

$$F_d = m_R g(1 + K_d) \quad (16)$$

where,  $K_d$  is the dynamic coefficient, represents the influence of dynamic loads applied to the launcher, with its value ranging between 2 and 3 based on practical experiences.

## 4. Discussion of Numerical simulation results

The numerical simulation is conducted in this section to analyze the dynamics of the proposed vehicle launcher system. At the beginning of the simulation, the initial conditions are established as follows:  $y_v = y_2 = y_5 = \varphi_L = \varphi_v = 0$  where  $\varphi_v$  and  $\varphi_L$  are the angular displacements of the vehicle and the launcher, respectively. The simulation time step is .01 s. First, the simulation is conducted when a force pulse is applied to the single tube launcher for a duration of 0.05 s to validate the model. Then the simulation is extended to examine the effect of multiple launches on system parts and initial disturbances of the unguided rockets

### 4.1. Model validation

The comparison of the angular displacement of the vehicle and launcher at  $\alpha_0 = 30^\circ$  between the proposed design and the reference model [12], which utilized the Lagrange equation, is depicted in Figure 5. The results from both methods exhibit a significant level of agreement.

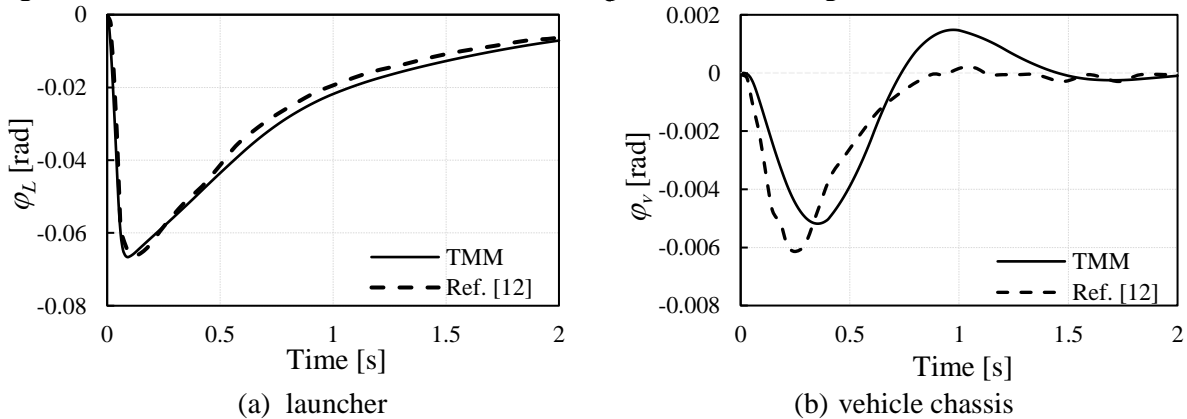


**Figure 5.** The launcher and vehicle angular displacement.

It is observed that the launcher angular displacement drops to  $-0.065$  rad abruptly and then takes more than 2 seconds to return to its initial position. This behavior will impact subsequent launches in a multiple-launch scenario and will be studied in the following subsections.

#### 4.2. Effect of multiple-launch on the dynamics of the system parts

In this section, the simulation extended to include firing a series of five rockets from tube one to tube five with a time delay between shots  $t_s=1s$  at  $\alpha_0 = 30^\circ$ . Figure 6 and Figure 7 illustrate the angular displacements and velocities of both the launcher and the vehicle. Figure 6 shows that the launcher angular velocity initially oscillates by a small amplitude that increases during successive launches, reaching a maximum angular displacement of  $\varphi_L = -0.065$  rad at the fifth shot. This indicates that the launcher vertical disturbance extensively increases as the vertical distance between the launch tubes (9) and the elevating mechanism trunnion (8) increases, causing the moment generated by the rocket motion through the launch tubes to increase. For the vehicle chassis (7), Figure 7 shows the vehicle angular velocity increases with each shot, reaching the peak after the fifth shot and the drop in angular displacement  $\varphi_v$  increases after each shot, peaking with the fifth shot. Figure 8 visually depicts the vertical linear displacements and velocity of the vehicle body mass center, whereas Figure 9 especially focuses on the vertical linear displacements and velocities of element 2 and element 5.

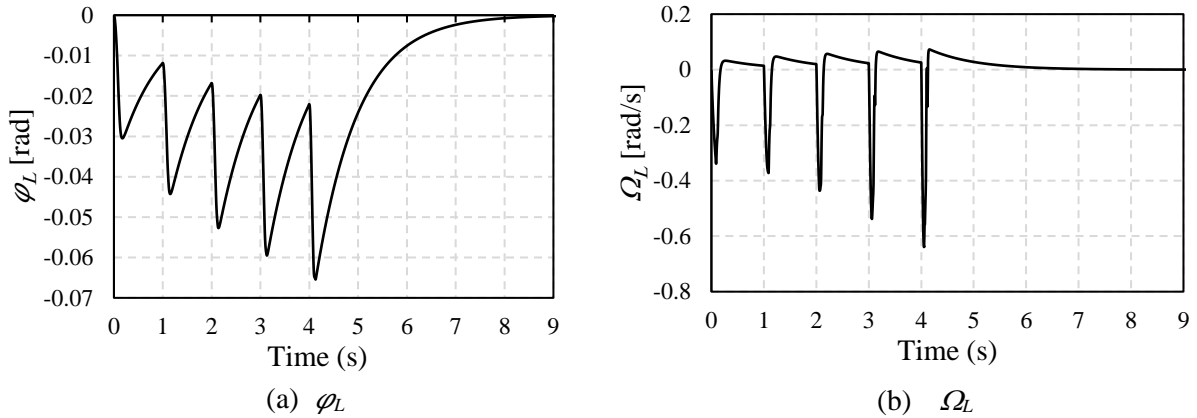


**Figure 6.** Angular displacement and velocity of the launcher.

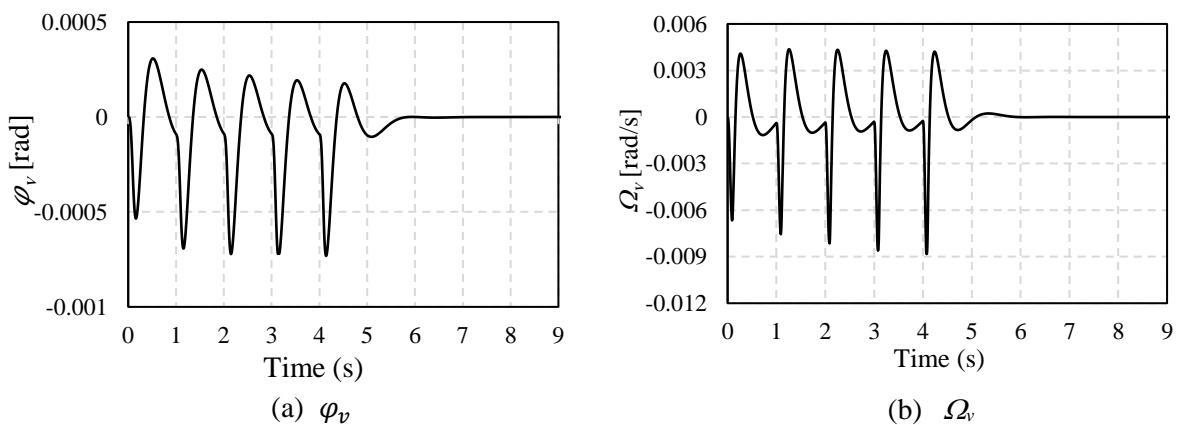
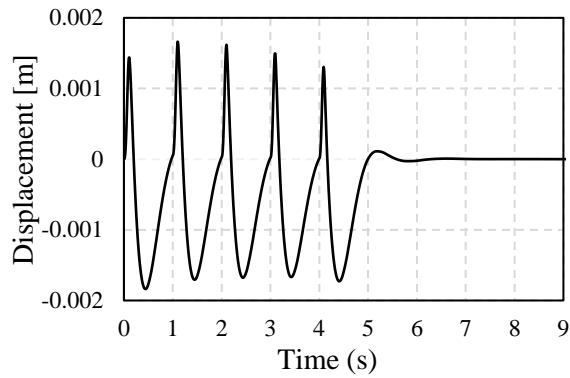
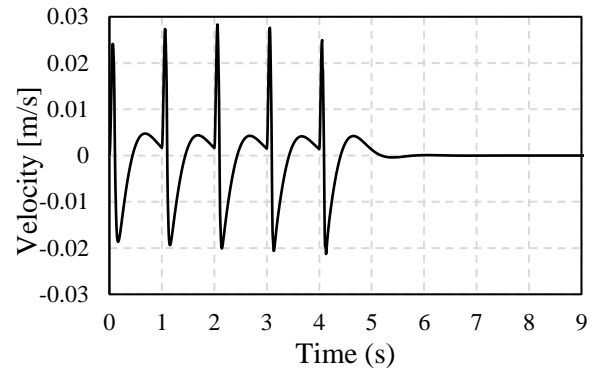


**Figure 7.** Angular displacement and velocity of the vehicle.



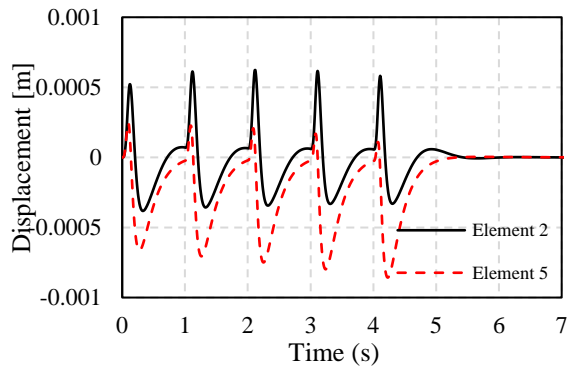


(a) vertical displacement

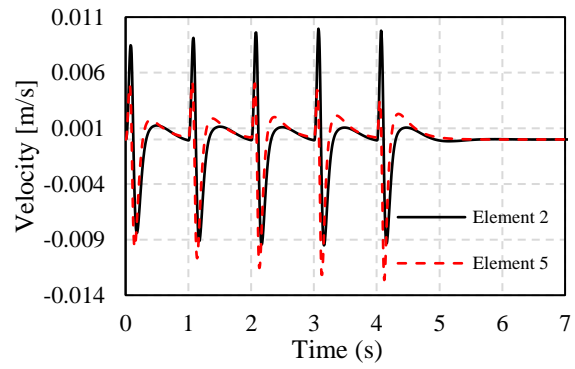


(b) velocity

**Figure 8.** Vertical displacement and velocity of vehicle mass center.



(a) vertical displacement



(b) velocity

**Figure 9.** Vertical displacement and velocity of elements 2 and 5.

#### 4.3. Effect of multiple launches on the initial parameters of unguided rocket

This section extends the simulation to examine the effects of multiple launches on the muzzle angular velocities and angular displacements of the rockets. A series of five rockets is fired varying three time delay between shots ( $t_s$ ) at  $\alpha_0 = 30^\circ$ . Table 2 shows the muzzle parameters of the launcher ( $\varphi_L$  and  $\Omega_L$ ) that affect the unguided rocket trajectory and dispersion when  $t_s = .4, .8$ , and  $1.2$  s. The average muzzle  $\varphi_L$  reduces as  $t_s$  increases, along with the standard deviation (STD) of muzzle  $\varphi_L$  and muzzle  $\Omega_L$ .

**Table 2.** Muzzle parameters of the rocket

$t_s$ [s]	parameter	shot1	shot2	shot3	shot4	shot5	Average	STD
0.4	$\varphi_L$ [rad]	-0.026	-0.052	-0.073	-0.090	-0.1	-0.069	0.03
	$\Omega_L$ [rad/s]	-0.23	-0.186	-0.138	-0.0935	-0.094	-0.148	.059
0.8	$\varphi_L$ [rad]	-0.026	-0.044	-0.056	-0.065	-0.072	-0.0530	0.018
	$\Omega_L$ [rad/s]	-0.23	-0.195	-0.15	-0.119	-0.125	-0.165	.047
1.2	$\varphi_L$ [rad]	-0.026	-0.039	-0.047	-0.05	-0.0601	-0.04	0.011
	$\Omega_L$ [rad/s]	-0.230	-0.200	-0.16	-0.130	-0.137	-0.17	0.037



## 5. Conclusion

Initial (launch) disturbances of MLRS have impact on dispersion of unguided rockets. This study provides a brief analysis of the dynamics of a multi-tube rocket launcher mounted on a wheeled vehicle. A mathematical dynamical model of the launcher vehicle system is established using the Transfer Matrix Method (TMM). This method facilitates modeling of the complex systems by eliminating the need to derive the overall dynamic equations. The findings demonstrate that multiple rocket launches notably influence various components of the system, with a pronounced effect on the angular motion of the elevating mechanism. This has a direct consequence on the muzzle parameters of unguided rockets, affecting their trajectory and consequently dispersion. Future studies could extend this research by evaluating additional launch scenarios and incorporating environmental variables to enhance the understanding of artillery system dynamics and further optimize launcher performance.

## References

- [1] Gu L, Rui X, Wang G, Yang F and Wei M 2020 A novel vibration control system applying annularly arranged thrusters for multiple launch rocket system in launching process, *Shock and Vibration*, vol. 2020, p. 7040827
- [2] Shabana A A 2020 *Dynamics of multibody systems* Cambridge university press
- [3] Chin S S 1961 *Missile configuration design*: McGraw-Hill
- [4] Cochran J E 1975 Investigation of factors which contribute to mallaunch of free rockets *NASA STI/Recon Technical Report N*, **76**, p. 33258
- [5] COCHRAN J and Christensen D 1981 Launcher/rocket dynamics and passive control in *7th Atmospheric Flight Mechanics Conference*, p. 1902
- [6] Şomoiaş P and Moldoveanu C E 2013 Numerical research on the stability of launching devices during firing, *Defence Technology*, **9**, pp 242-248
- [7] Dokumaci K, Aydemir M T and Salamci M U 2014 Modeling, PID control and simulation of a rocket launcher system in *2014 16th International Power Electronics and Motion Control Conference and Exposition* pp 1283-1288
- [8] Li B, Rui X and Wang G 2022 A simplified dynamic model and control for a multiple launch rocket system *Journal of Vibration and Control*, **28**, pp 2288-2300
- [9] Dziopa Z, Krzysztofik I and Koruba Z 2010 An analysis of the dynamics of a launcher-missile system on a moveable base *Bulletin of the Polish Academy of Sciences Technical Sciences*, pp 645-650-645-650
- [10] Li B, Rui X, and Zhou Q 2018 Study on simulation and experiment of control for multiple launch rocket system by computed torque method *Nonlinear Dynamics*, **91**, pp1639-1652
- [11] Li B and Rui X 2018 Vibration control of uncertain multiple launch rocket system using radial basis function neural network, *Mechanical Systems and Signal Processing*, **98**, pp. 702-721
- [12] Fedaravičius A, Jass K., Gaidys R, and Pilkauskas K 2023 Dynamics of the Missile Launch from the Very Short-Range Mobile Firing Unit *Shock and Vibration* vol. 2023, p. 3082704
- [13] Rui X, Yun L, Lu Y, He B and Wang G 2008 Transfer matrix method of multibody system and its applications *Science, Beijing, China*, pp. 101-138
- [14] Rui X, Bestle D, Zhang J and Zhou Q 2016 A new version of transfer matrix method for multibody systems *Multibody System Dynamics*, **38**, pp 137-156
- [15] Zhan Z H, Rui X, Rong B, Yang F and Wang G 2011 Design of active vibration control for launcher of multiple launch rocket system *Proceedings of the Institution of Mechanical Engineers, Part K Journal of Multi-body Dynamics*, **225**, pp. 280-293,.
- [16] Tang W, Rui X, Wang G, Rui X, Song Z and Gu L 2016 Dynamics design for multiple launch rocket system using transfer matrix method for multibody system *Proceedings of the Institution of Mechanical Engineers, Part G Journal of Aerospace Engineering*, **230**, pp 2557-2568,.

- [17] Li B, Rui X, Zhou Q, Zhang J and Gu L 2018 Modeling, simulation and experiment of multibody system launch dynamics for multiple launch rocket system in *International Design Engineering Technical Conferences and Computers and Information in Engineering Conference*, p. V006T09A068.
- [18] Li B, Rui X, Wang G, Zhang J and Zhou Q 2021 On modeling and dynamics of a multiple launch rocket system *Proceedings of the Institution of Mechanical Engineers, Part G Journal of Aerospace Engineering*, **235**, pp. 1664-1686
- [19] Eisa H, Ahmed M, Khalil M and Saleh S 2024 Dynamic behavior of a wheeled rocket launcher using transfer matrix method of multibody system in *Journal of Physics: Conference Series*, p. 012034.
- [20] Rui X, Zhang J and Zhou Q 2014 Automatic deduction theorem of overall transfer equation of multibody system *Advances in Mechanical Engineering*, **6**, p. 378047
- [21] Jazar R N 2008 *Vehicle dynamics* **1** Springer
- [22] Khalil M, Abdalla H and Kamal O 2009 Trajectory prediction for a typical fin stabilized artillery rocket in *International conference on aerospace sciences and aviation technology* pp. 1-14.